Rheol Acta 37:289–298 (1998)

ORIGINAL CONTRIBUTION

Bruno Souloumiac
Michel Vincent

Steady shear viscosity of short fibre suspensions in thermoplastics

Received: 22 September 1997
Accepted: 5 March 1998

B. Souloumiac · M. Vincent (✉)
Centre de Mise en Forme des Matériaux
UMR CNRS 7635
Ecole des Mines de Paris
BP 207
06904 Sophia-Antipolis Cedex, France

Abstract The rheological behaviour of a polyethylene, two polyamides and a silicone oil filled with different fibre contents are studied in capillary rheometry. The viscosity increase induced by the fibres is important for the silicone oil, and negligible for the polyethylene. The polyamide is intermediate. The same classification stands for the pressure loss in the convergent channel upstream from the capillary. A constitutive equation based on a cell model which takes into account the shear-thinning behaviour of the matrix is built. The predictions of the model are in correct agreement with the measurements.

Key words Reinforced thermoplastics – viscosity – convergent channel – shear-thinning – fibre suspension

Introduction

Short fibre reinforced thermoplastics present improved mechanical properties, and they can be processed with the same equipment as neat materials. Nevertheless, flow induced fibre orientation leads to anisotropic mechanical properties, so that the moulded component quality is not as high as expected. The effect of the fibres on the flow velocity and stress fields is also important. Therefore, the anisotropic rheological properties must be accurately described, both experimentally, and by means of constitutive equations taking into account the microstructure.

Numerous studies with various materials have shown that the shear viscosity is increased by the addition of fibres. The effect is more pronounced at low shear rate (Kitano and Kataoka, 1980; Crowson et al., 1980; Crowson and Folkes, 1980; Becraft and Metzner, 1992; Kamal and Mutel, 1985). The Newtonian plateau tends to disappear when the fibre content increases (Crowson et al., 1980; Czarnecki and White, 1980), especially with large aspect ratio fibres or at high concentration. The relative viscosity, ratio of the viscosity of the suspension to the viscosity of the matrix, usually decreases with the shear rate, and can reach the value 1 (Kitano and Kataoka, 1980; Crowson et al., 1980). The relative viscosity is an increasing function of the fibre aspect ratio (Kitano and Kataoka, 1980; Kitano et al., 1981, 1984; Laun, 1984). The studies on the behaviour in elongational situations are of course less numerous, but it is admitted that the increase of the elongational viscosity is much more important than the shear viscosity (Laun, 1984; Mewis and Metzner, 1974; Kamal et al., 1984).

All these observations can be explained by the fibre structure. In shear flows, fibres are mainly oriented in the flow direction and their contribution to the stress is small. The degree of orientation depends on the flow geometry (fibre-wall interactions), fibre concentration (fibre-fibre interactions) and aspect ratio, and on the rheological properties of the matrix (viscosity, elasticity). In elongational flows, fibres get oriented in a stable position in the direction of extension, so that they have a large influence on the elongational viscosity.

Behaviour laws consist of two equations. The first one concerns fibre orientation. The equations describing the motion of a single particle in a Newtonian fluid were introduced by Jeffery (1922). This work has been extended to account for fibre interactions using an

RA 888

analogy with rotary Brownian diffusion (Folgar and Tucker, 1984; Ranganathan and Advanti, 1991; Kamal and Mutel, 1989). The second one is the expression of the stress. In most works, the fluid is Newtonian. Following the work of Hand (1962) on the general form of the extra stress tensor, and using Jeffery's solution (1922) for the stress field around a single particle, Lispcomb et al. (1988) obtained a continuum theory for dilute suspensions of large aspect ratio particles. Phan-Thien and Graham (1991) modified the general form of the stress tensor to extend the theory to the semi-dilute regime. Dinh and Armstrong (1984) developed an equation for semi-concentrated fibre suspensions, using a cell model approach (Batchelor, 1970) which has a similar general form. The theoretical predictions agree reasonably well with rheological experiments (Bibbo et al., 1985; Ganani and Powel, 1986; Ausias et al., 1992). Extensions to an Ellis behaviour law have been proposed by Wang and Cheau (1991). Shaqfeh and Fredrickson (1990) used slender body theory and a multiple scattering expansion to represent the hydrodynamic interactions between the fibres. Ranganathan and Advani (1991) extended the previous work to account for finite length fibres. Becraft and Metzner (1992) started from a different background. They used the molecular theory of Doi (1981) for concentrated suspensions of rodlike molecules, modified by Doraiswamy and Metzner (1986). Aït-Kadi and Grmela (1994) built a rheological model for fibre suspensions in viscoelastic media.

The objectives of this work are first to obtain rheological data for different reinforced thermoplastics in capillary rheometry, with a special attention to the convergent channel upstream the capillary where both elongational and shear deformations take place. Second, a constitutive equation for fibre suspensions is presented. In order to make it suitable for process modelling, the shear-thinning behaviour of the matrix is taken into account. The predictions of the model are compared to the measurements.

Experiments

Materials and experimental conditions

Three different glass fibre reinforced thermoplastic polymers have been used (Table 1):

- a high density polyethylene provided by Solvay, without fibres, and reinforced with 20 wt.% glass fibre. By mixing in a capillary rheometer at 220 °C the reinforced polymer with the matrix, three intermediate fibre contents were obtained;
- a polyamide 66, provided by BASF, reinforced with 30 wt.% (Ultramid A3G6) and 50 wt.% (Ultramid A3G10) fibre, as well as the unifilled matrix.
- a polyamide 66 provided by Nyltech, reinforced with 35 wt.% (A216V35) and 50 wt.% (A216V50), as well as the unfilled matrix.

In addition, a silicone oil filled with 1, 4 and 8 vol.% polyamide fibres with narrow length distribution has been tested. Unlike thermoplastic polymers, the silicone oil is nearly Newtonian: under 100 s^{-1} its viscosity at room temperature is constant equal to 9.5 Pa s, and above it becomes slightly shear-thinning, with a power-law index of 0.82 at 1000 s^{-1}. Moreover, no elasticity has been detected with a cone and plate rheogoniometer.

Table 1 summarises the characteristics of the materials, and Fig. 1 shows the fibre length distribution, measured after burning the thermoplastic matrix. The mixing operation of the reinforced and neat polyethylenes did not affect the fibre length distribution.

The 2 vol.% reinforced polyethylene and the 1 vol.% silicone oil are in the semiconcentrated regime ($\Phi < 2R/L$, with Φ the fibre concentration, R the fibre radius and L the average length). The other materials are concentrated suspensions.

We used a Rheoplast capillary rheometer (Villemaire and Agassant, 1984) where the material is pre-sheared in a Couette geometry before capillary measurements. The capillary diameters are 0.93, 1.39 and 3 mm, and the length over diameter ratios are 0, 4, 8 and 16. The pressure loss in the convergent channel upstream from the capillary is determined by the classical Bagley corrections. This convergent channel has a 90° angle, its diameter is 16 mm at the entrance.

Experiments were carried out at 220 °C for the polyethylenes, at 290 °C for the polyamides (after drying in a vacuum oven for 16 h at 100 °C), and at 20 °C for the silicone oil.

No inhomogeneity of fibre concentration in the cross-section of the extrudates at the exit of the capillary has been observed for the thermoplastic polymers.

Table 1 Description of the materials (for the polyamides, the two fibre lengths correspond to the two fibre contents)

	Fibre content (weight %)	Fibre content (volume %)	Fibre diameter (μm)	Mean fibre length (μm)	Fibre aspect ratio
Polyethylene	0–6–11–16–20	0–2–4–6–8	15	500	33
Polyamide BASF	0–30–50	0–16–31	7	163–194	23–28
Polyamide Nyltech	0–35–50	0–20–31	7	141–128	20–18
Silicone oil		0–1–4–8	18	660	37

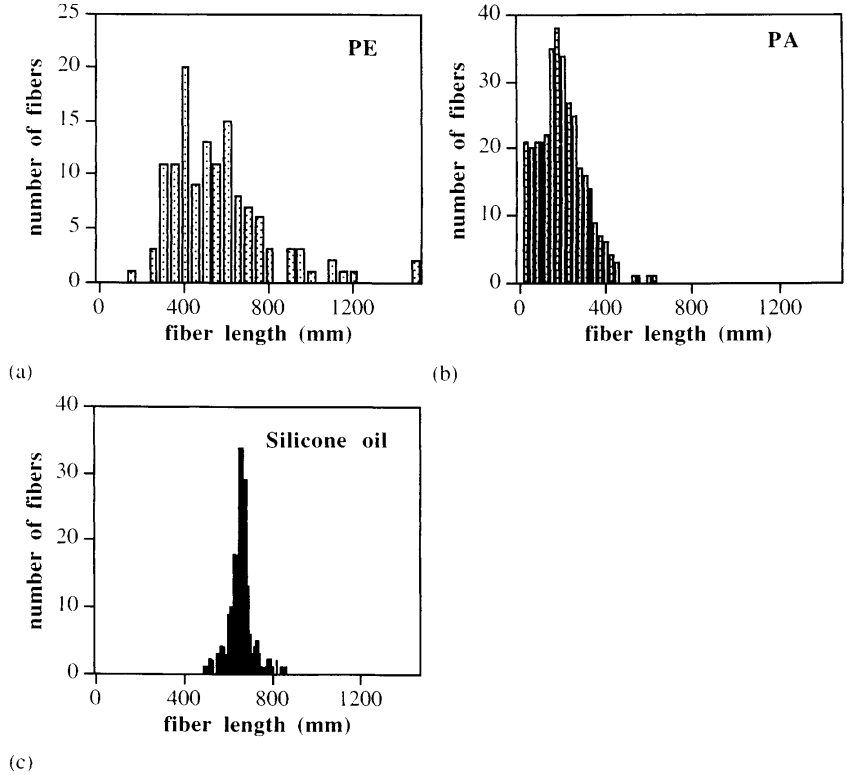

Fig. 1 Fibre length distribution in the granules of polyethylene (a) and polyamide (BASF, 31 vol.%) (b). Polyamide fibres used with the silicone oil (c)

Viscosity

For all the materials, the Bagley plots are linear. Flow curves obtained with different capillary diameters are identical, which is an indication that there is no wall slippage.

All thermoplastic polymers have a shear-thinning behaviour. Figure 2 shows the viscosity curves of the matrix materials, and Table 2 gives the consistency and average power-law indexes. This index does not change significantly with the addition of fibres. Figure 3a shows the relative viscosity (ratio of the viscosity of the filled and unfilled polymer at the same shear rate) for the Nyltech polyamides. Viscosity increases with the fibre content. The relative viscosity is nearly constant under 2000 s^{-1}, and above it decreases. The BASF polyamide (not shown) and the filled silicone oil (Fig. 3b) have similar behaviours. On the contrary, the polyethylene viscosity is nearly constant, whatever the fibre content. Figure 4 summarises the evolution of the reduced viscosity (taken at the plateau around 500–1000 s^{-1}, see Fig. 3) with the volume fibre content. The sensitivity to the fibre content depends strongly on the matrix.

These results can be related to the fibre orientation. In a Newtonian fluid, a single fibre rotates, but spends most of the time nearly oriented in the flow direction. When fibres interact, the rotations are perturbed, but still exist (Folgar and Tucker, 1984). In a viscoelastic fluid, the elasticity tends to stabilise the fibres in the flow direction (de Bonhome et al., 1990). In the highly elastic polyethylene, fibres may be well oriented, and their contribution to the pressure is low. On the contrary, the silicone oil is almost inelastic, and the degree of orientation is certainly lower. Polyamides are in the intermediate range.

Pressure loss in the convergent channel

We assume that the end pressure losses determined from the Bagley plots are mostly associated to entrance effects. Figure 5 shows the evolution of the pressure loss with the flow rate. The pressure loss increases with the fibre content. This is due to the fact that the rigid fibres, which are well oriented in the flow direction, resist the elongational deformations ("hardening effect").

Next results are shown in terms of relative pressure loss in the convergent channel, defined as the ratio of the pressure loss for the reinforced material, to the pressure loss for the unreinforced one at the same flow rate. Figure 6 shows that when the apparent shear rate in the capillary ($4Q/\pi R_c^3$, with Q the flow rate and R_c the capillary radius) decreases, the relative pressure loss increases: the contribution of the fibres increases. This could be the effect of the shear-thinning behaviour of

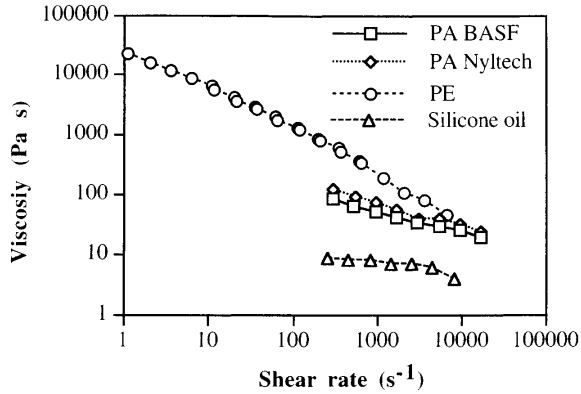

Fig. 2 Viscosity of the matrix materials

Table 2 Rheological characteristics of the matrices

Material	Power-law index	Consistency (Pa s^m)
Polyethylene 220 °C	0.34	27000
Polyamide BASF 290 °C	0.58	900
Polyamide Nyltech 290 °C	0.56	1480
Silicone oil 20 °C	0.82	24

the polymer: even in elongational situations, the polymer is submitted to local shear deformations between the fibres. At high apparent shear rate in the capillary, the local viscosity in the suspension is lower than the viscosity of the polymer without fibres in the same situation. The "hardening" effect of the fibres is partly counteracted by the shear-thinning behaviour of the matrix. At low apparent shear rate, the polymer is nearly Newtonian, the local viscosity in the suspension is of the same order as the viscosity without fibres, and the "hardening" effect of the fibre is maximum. This explanation is supported by the fact that at high fibre content the pressure loss vs. flow rate curves (Fig. 5) are well fitted by a line with a slope equal to the power-law index of the matrix (in a logarithmic plot).

Figure 7 shows that the relative pressure loss increases with the fibre content. This shows again clearly the "hardening" effect of the fibres in elongational situations. The contribution of the fibres to the pressure loss is small, but not negligible for the polyethylene (Fig. 7a), high for the silicone oil (Fig. 7c), and intermediate for the polyamide (Fig. 7b). So the classification is the same as for the relative viscosity, but the effect is much more important: the relative viscosity was always below 2 (Fig. 4), whereas the relative pressure loss exceeds 6 for the silicone oil.

Behaviour law

The objective is to build a stress expression which takes into account the shear-thinning behaviour of the matrix, represented by a power-law. We will determine the contribution of the fibres to the stress field using a cell model. The development assumes that hydrodynamic interactions between the fibres are weak, which is of course an important assumption for the suspensions mentioned before.

The fibre of radius R is in a cell of radius h (Fig. 8). Along the boundary of the cell ($r=h$), the relative velocity of the fluid with respect to the fibre, $\boldsymbol{W}(s)$, is supposed to be undisturbed by the particle. s is a coordinate with reference to the centre of the fibre. Assuming that the velocity gradient $\nabla\boldsymbol{u}$ is constant along a fibre, $\boldsymbol{W}(s)$ is given by:

$$\boldsymbol{W}(s) = W(s)\,\boldsymbol{p} = s(\nabla\boldsymbol{u} : [\boldsymbol{pp}])\,\boldsymbol{p} \qquad (1)$$

where $\boldsymbol{p}$ is a unit vector in direction of the fibre, and $\boldsymbol{pp}$ is the tensor product (component $(\boldsymbol{pp})_{ij}=p_i p_j$). Assuming a sticking contact at the surface of the fibre, the fluid velocity in the cell is:

$$w(r) = W(s)\,\frac{r^{(m-1)/m} - h^{(m-1)/m}}{h^{(m-1)/m} - R^{(m-1)/m}} \qquad (2)$$

where m is the power-law index of the matrix. The shear stress at the fibre surface σ_{rz} is therefore:

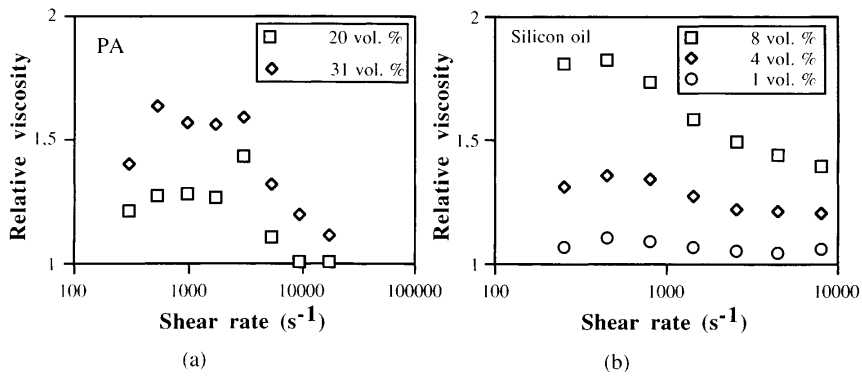

Fig. 3 Relative viscosity vs. shear rate measured in capillary rheometry for (a) the polyamide Nyltech and (b) the silicone oil

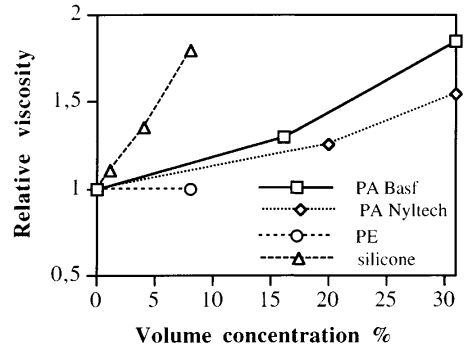

Fig. 4 Influence of the fibre concentration on the relative viscosity

$$\sigma_{rz} = K\left\{\frac{1-m}{mR\left[1-\left(\frac{R}{h}\right)^{(1-m)/m}\right]}\right\}^{m} \times |W(s)|^{(m-1)}\, W(s)\, ds \qquad (3)$$

where K is the matrix consistency. The force exerted by the fluid on a length ds of fibre is:

$$df(s) = 2\pi R\sigma_{rz} \qquad (4)$$

The force exerted by the fluid on the fibre between s and the tip ($s=L/2$, where L is the fibre length) is:

$$f(s) = \int_{s}^{L/2} df(\tau) \qquad (5)$$

and the force vector is $\boldsymbol{f}(s)=f(s)\boldsymbol{p}$. The stress tensor on the surface of the fibre at s is: $\frac{f(s)}{\pi R^2}\,\boldsymbol{pp}$, and the average along the fibre length is:

$$\langle\boldsymbol{\sigma}_{f_i}\rangle = \frac{2}{L\pi R^2}\int_{0}^{L/2} f(s)\,\boldsymbol{p}_i\boldsymbol{p}_i\, ds \qquad (6)$$

where the subscript i has been added to refer to the number of the considered fibre. In a given volume V containing a large number N of fibres, each one having a volume V_0, the contribution of the fibres to the stress tensor is the sum of the contribution of each fibre, $<\boldsymbol{\sigma}_{f_i}>$:

$$\langle\boldsymbol{\sigma}_f\rangle = \sum_{i=1}^{N}\frac{V_0}{V}\langle\boldsymbol{\sigma}_{f_i}\rangle \qquad (7)$$

or

$$\langle\boldsymbol{\sigma}_f\rangle = \Phi\int_{\boldsymbol{p}}\Psi(\boldsymbol{p},t)\langle\boldsymbol{\sigma}_{f_i}\rangle d\boldsymbol{p} \qquad (8)$$

where Φ is the fibre concentration, and Ψ the fibre orientation distribution function. Finally, after integration of Eq. (6), we obtain:

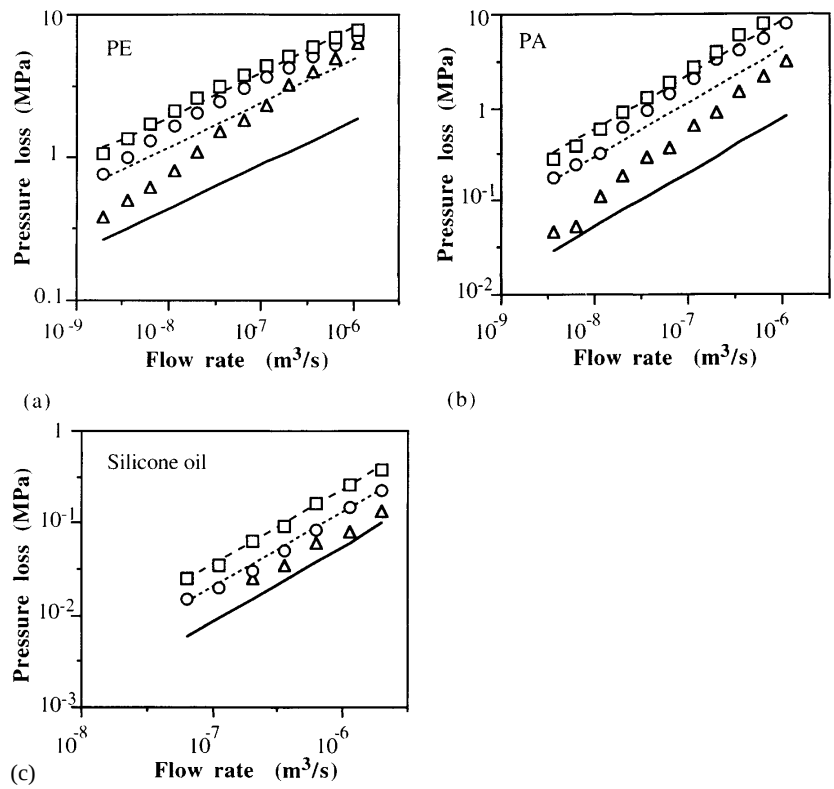

Fig. 5 Pressure loss in the convergent channel vs. flow rate for (a) polyethylene (capillary diameter: 1.39 mm), (b) polyamide BASF (capillary diameter 0.93 mm), (c) silicone oil (capillary diameter 1.39 mm). Symbols: measurements. Lines: calculation. ——, △: unfilled (PE, PA), 1% (silicone oil). - - - -, ○: 4% (polyethylene, silicone oil) or 16% (polyamide). – – –, □: 8% (polyethylene, silicone oil), 31% (polyamide)

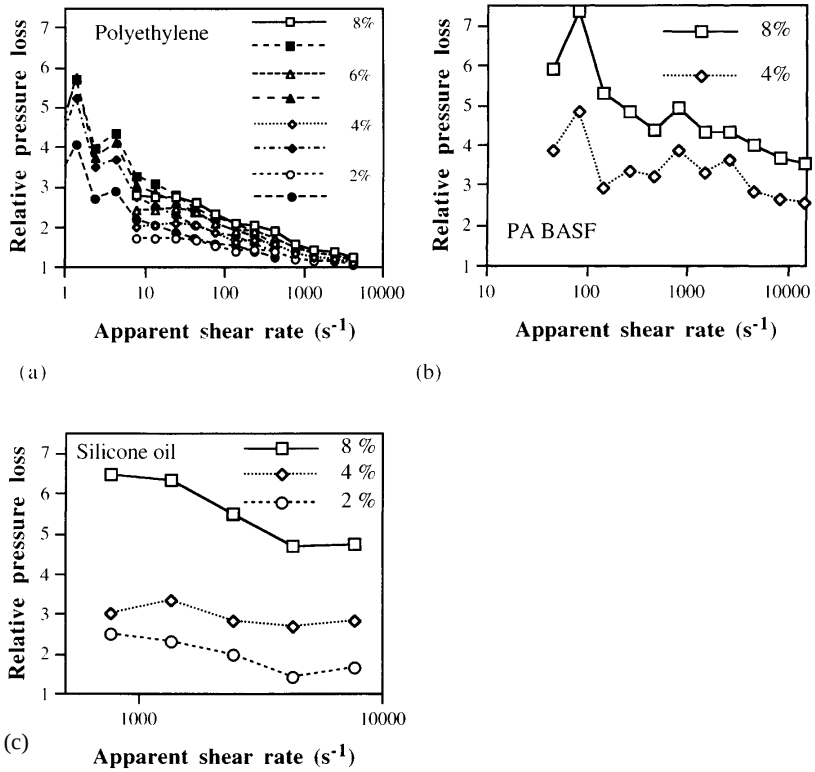

Fig. 6 Relative pressure loss vs. apparent shear rate in the capillary. (a) Polyethylene, capillary diameters 1.39 (open symbols) and 3 mm (black symbols). (b) Polyamide (Ultramid), capillary diameter 0.93 mm. (c) Silicone oil, capillary diameter 1.39 mm

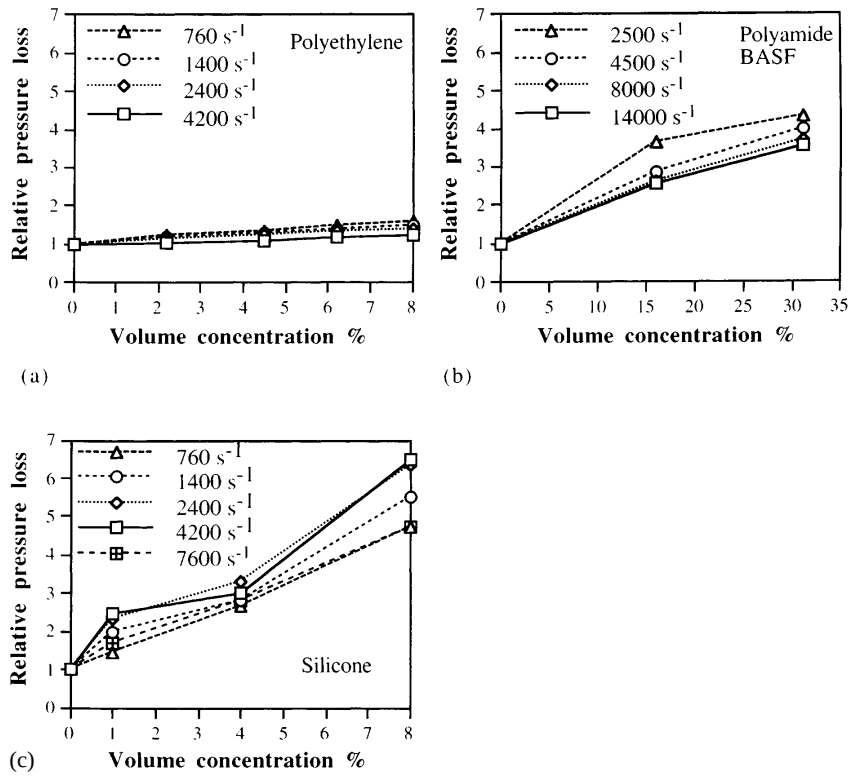

Fig. 7 Relative pressure loss vs. volume concentration for: (a) the polyethylene (capillary 1.39 mm), (b) the polyamide BASF (capillary 0.93 mm), (c) the silicone oil (capillary 1.39 mm)

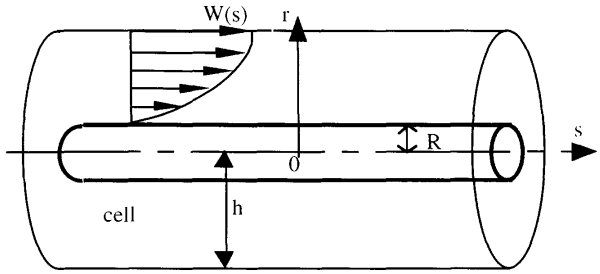

Fig. 8 Geometry of the cell surrounding a fibre

$$\langle \boldsymbol{\sigma}_f \rangle = \frac{2\Phi K \beta^{m+1}}{m+2} \left(\frac{1-m}{m\left(1-(R/h)^{(1-m)/m}\right)} \right)^m \times \int_p \Psi(\boldsymbol{p},t) |\nabla \boldsymbol{u} : \boldsymbol{pp}|^{m-1} (\nabla \boldsymbol{u} : \boldsymbol{pp}) \, \boldsymbol{pp} \, d\boldsymbol{p} \quad (9)$$

The total stress field $<\boldsymbol{\sigma}>$ is the sum of the contribution of the fibres, $<\boldsymbol{\sigma}_f>$, and of the matrix (Batchelor, 1970). The homogenisation of the matrix contribution with a non-linear power-law is not straightforward, and we assume the same power-law as for unreinforced polymers:

$$\langle \boldsymbol{\sigma} \rangle = -P' \boldsymbol{I} + 2K (2 I_2)^{\frac{m-1}{2}} \dot{\boldsymbol{\varepsilon}} + \langle \boldsymbol{\sigma}_f \rangle \quad (10)$$

where $\boldsymbol{I}$ is the identity tensor, and I_2 is the second invariant of the rate of strain tensor $\dot{\boldsymbol{\varepsilon}}$, defined as $\sum_{i,j} \dot{\varepsilon}_{ij}^2$.

If m tends to 1, Eq. (10) reduces to the expression found by Dinh and Armstrong (1984). This result is in agreement with the work of Goddard (1976), who found that for aligned fibres in a uniaxial extension of a power-law fluid, the stress is proportional to β^{m+1}.

An important unknown parameter is the radius of the cell h. Different choices have been made, the average interfibre spacing (Batchelor, 1971) or the average closest approach distance between a fibre and its nearest neighbour (Dinh and Armstrong, 1984). Hydrodynamic screening lengths have been discussed by Shaqfeh and Fredrickson (1990) and Mackaplow and Shaqfeh (1996), for semi-dilute suspensions in Newtonian fluids. Here, we will test the sensitivity of our results to h. The minimum value of h is R, when two fibres are in contact (the previous analysis is of course no longer valid). The maximum of the average value of h, $h_{\max}$, is reached when all the fibres are aligned. Supposing for instance a square arrangement, the number of fibres n per unit volume is:

$$n = \frac{1}{h_{max}^2 L} \quad (11)$$

Introducing the fibre concentration $\Phi = n\pi R^2 L$, $h_{\max}$ becomes:

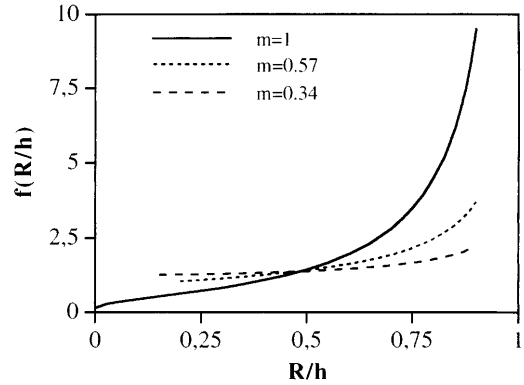

Fig. 9 Influence of the cell dimension h on the function f as defined in Eq. (13)

$$h_{max} = R\sqrt{\frac{\pi}{\Phi}} \quad (12)$$

$h_{\max}$ has the same scaling with Φ than the average interfibre spacing. For instance, for fibres of length $L = 100$ μm and diameter $2R = 10$ μm, and a fibre concentration of 8%, h is included between 5 and 31 μm.

Let us define the coupling coefficient μ_m appearing in Eq. (9) as:

$$\mu_m = \frac{2\Phi K \beta^{m+1}}{m+2} \left(\frac{1-m}{m\left(1-(R/h)^{(1-m)/m}\right)} \right)^m = \frac{2\Phi K \beta^{m+1}}{m+2} f\left(\frac{R}{h}\right) \quad (13)$$

Figure 9 shows the evolution of the function f for $m = 0.57$ and $m = 0.34$, corresponding respectively to the values of the power-law index of the polyamide and polyethylene. The curve corresponding to $m = 1$ is the limit when m tends to 1:

$$f\left(\frac{R}{h}\right) = \left(ln\left(\frac{h}{R}\right)\right)^{-1} \quad (14)$$

The dependence of μ_m to the cell dimension decreases when the power-law index decreases. This can be explained by the fact that the velocity gradient is more and more concentrated near the fibre, so that the volume of fluid perturbed by the fibre is less important. Therefore, it is reasonable to take $h = R\sqrt{\frac{\pi}{\Phi}}$.

Figure 10 a shows that the rate of change of the coupling coefficient with the fibre aspect ratio decreases with the power-law index m. This is a favourable result for actual reinforced thermoplastics with non constant fibre length (see Fig. 1). Figure 10 b shows the same trend for the volume concentration.

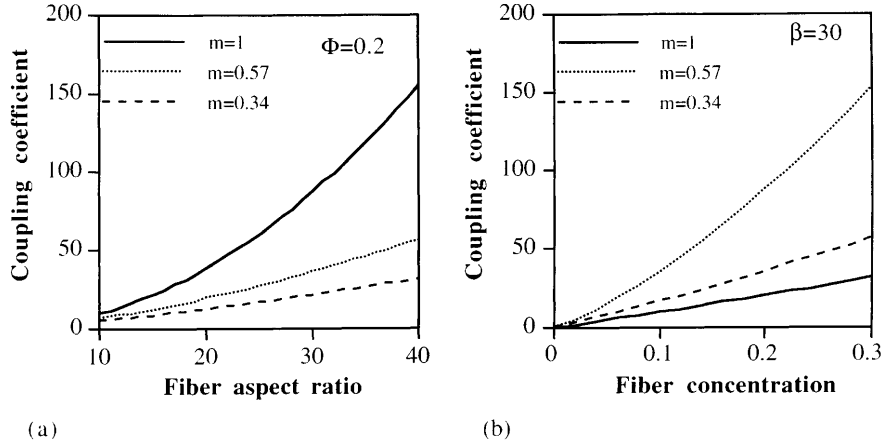

Fig. 10 Influence of: (a) the fibre aspect ratio (for a volume fraction of 0.2); (b) the fibre concentration (for an aspect ratio of 30), on the coupling coefficient for different values of the power-law index *m*

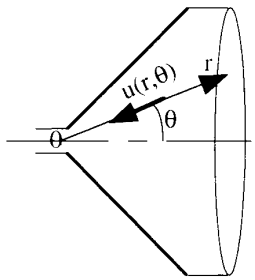

Fig. 11 Geometry of the convergent channel

Comparison between experiments and computation

We will focus on the pressure losses in the convergent channel. It should have been possible to study also the shear viscosity, but this is very sensitive to the fibre orientation description: the viscosity increase is directly related to the degree of alignment of the fibres in the flow direction. The comparison should have ended with a check of the validity of orientation equations.

Figure 11 shows the geometry of the convergent channel. In spherical coordinates, we assume that the velocity vector has only one component along the radial axis $u(r,\theta)$. Fibres are supposed to be oriented parallel to the velocity field. This assumption is justified, because experimental observations have shown that, in a convergent channel, extensional deformations orient fibres in the flow direction (Vincent and Agassant, 1991). It has been used by Lipscomb et al. (1988), who obtained an excellent agreement between experimental data for a dilute suspension in a Newtonian fluid and the calculation based on the behaviour law described by the authors. Moreover, Harlen and Koch (1992) showed that increasing extensional viscosity of non shear-thinning fluid subjected to purely elongational flow reduces hydrodynamic dispersion. The fully coupled problem requires much more complex numerical resolution (Ranganathan and Advani, 1991; Papanastasiou and Alexandrou, 1987; Ausias et al., 1994; Tang and Altan, 1995). The largest error is at the entrance of the channel, where fibres can arrive with completely different orientations, but this is not very important because the pressure loss mainly takes place at the end of the geometry. A fully coupled finite element simulation has shown the validity of this hypothesis (Souloumiac, 1996). The material is assumed to be incompressible. The equilibrium equation, neglecting gravity and inertia, applied to Eq. (10), leads to a third order differential equation with the velocity as unknown. After numerical resolution, the pressure loss is determined.

Figure 5 compares the predicted and measured pressure losses for the different materials. For the unfilled polyamide and polyethylene, the difference between calculation and measurement is quite large. The power-law is unable to predict the pressure loss in a convergent channel where viscoelasticity plays an important role. For all the materials, when the fibre content increases, the difference decreases, and the agreement becomes very good at the highest concentrations. This means that the "hardening" effect of the fibres, and the shear dominated flow around a test fibre in a situation where elongation is important overcomes the viscoelastic nature of the polymer. The agreement for the inelastic silicone oil is always correct, except at low flow rate for the 1% suspension. In this case, the measured pressures are very low, and the precision of the measurement is not so good.

Finally, the model permits to find the correct dependence of the pressure loss with the flow rate, that is a slope close to the power-law index in a logarithmic plot. The quality of the agreement between experiments and computations using a behaviour law which neglects hydrodynamic interactions could seem surprising. This could be due to the flow situation with well oriented fibres, in which the "hydrodynamic screening" (fibres close to the test fibre reduce the effect of farther fibres)

is effective (Batchelor, 1971; Shaqfeh and Koch, 1990). Other flow geometries with more important contributions of shear deformation could lead to lower quality results.

Conclusions

The viscosity enhancement caused by the fibres depends on the matrix. The elasticity level, as well as the shear-thinning behaviour are partly responsible for these differences. The same result stands for the pressure loss in a convergent channel. The shear-thinning anisotropic behaviour law shows that the sensitivity to the cell dimension and to the fibre aspect ratio decreases when the power-law index decreases. This is a favourable point because these two parameters are variable in a fibre suspension. The predictions of the model agree well with the measured pressure losses in the convergent channel, even for concentrated suspensions.

Acknowledgements This work was partly supported by the Commission of the European Community in the framework of a Brite-Euram project (BE8081), and by Institut Français du Pétrole, Gaz de France and Solvay. We would like to thank M. Muncker and M.-Ph. Toitgans for their help in rheological measurements.

References

Ait-Kadi A, Grmela M (1994) Modelling the rheological behaviour of fibre suspensions in viscoelastic media. J Non-Newt Fluid Mech 53:65–81

Ausias G, Agassant JF, Vincent M, Lafleur PG, Lavoie PA, Carreau PJ (1992) Rheology of short glass fiber reinforced polypropylene. J Rheol 36(4):525–542

Ausias G, Agassant JF, Vincent M (1994) Flow and fiber orientation calculations in reinforced thermoplastic extruded tubes. Intern Polym Proc 9:51–59

Batchelor GK (1970) The stress system in a suspension of force free particles. J Fluid Mech 41:545–570

Batchelor GK (1971) The stress generated in a non-dilute suspension of elongated particles by pure straining motion. J Fluid Mech 46:813–829

Becraft ML, Metzner AB (1992) The rheology, fiber orientation, and processing behavior of fiber-filled fluids. J Rheol 36:143–174

Bibbo MA, Dinh SM, Armstrong RC (1985) Shear flow properties of semiconcentrated fiber suspensions. J Rheol 29:905–929

Crowson RJ, Folkes MJ, Bright PF (1980) Rheology of short glass fiber-reinforced thermoplastics and its application to injection molding. I. Fiber motion and viscosity measurement. Polym Eng Sci 20:925–933

Crowson RJ, Folkes MJ (1980) Rheology of short glass fiber-reinforced thermoplastics and its application to injection molding. II. The effect of material parameters. Polym Eng Sci 20:934–940

Czarnecki L, White JL (1980) Shear flow rheological properties, fiber damage, and mastication characteristics of aramid-, glass-, and cellulose-fiber-reinforced polystyrene melts. J Appl Polym Sci 25: 1217–1244

de Bonhome G, de Brouwer T, Keunings R, Peiti C, Agassant JF, Vincent M (1990) A microrheological study of fiber suspensions. 6th Annual Meeting of the Polymer Processing Society, Nice, France

Dinh SM, Armstrong RC (1984) A rheological equation of state for semiconcentrated fiber suspension. J Rheol 28:207–227

Doi M (1981) Molecular dynamics and rheological properties of concentrated solutions of rodlike polymers in isotropic and liquid crystalline phases. J Polym Sci Polym Phys Ed 19:229–243

Doraiswamy D, Metzner AB (1986) The rheology of polymeric liquid crystals. Rheol Acta 25:580–587

Folgar F, Tucker CL (1984) Orientation behavior of fibers in concentrated suspensions. J Reinf Plastics Compos 3:98–119

Ganani E, Powell RL (1986) Rheological behavior of rodlike particles in Newtonian and non-Newtonian fluids. J Rheol 30:995–1013

Goddard JD (1976) The stress field of slender particles oriented by a non-Newtonian extensional flow. J Fluid Mech 78:177–206

Hand GL (1962) A theory of anisotropic fluids. J Fluid Mech 13:33–46

Harlen OG, Koch DL (1992) Extensional flow of a suspension of fibers in a dilute polymer solution. Phys Fluid 4:1070–1073

Jeffery GB (1922) The motion of ellipsoidal particles immersed in a viscous fluid. Proc Roy Soc London A 102:161–179

Kamal MR, Mutel AT (1985) Rheological properties of suspensions in Newtonian and non-Newtonian fluids. J Polym Eng 5:293–382

Kamal MR, Mutel AT (1989) The prediction of flow and orientation behavior of short fiber reinforced melts in simple flow systems. Polym Compos 10:337–343

Kamal MR, Mutel AT, Utracki LA (1984) Elongational behavior of short glass fiber reinforced polypropylene melts. Polym Compos 5:289–298

Kitano T, Kataoka T (1980) The effect of the mixing methods on viscous properties of polyethylene melts filled with fibres. Rheol Acta 19:753–763

Kitano T, Kataoka T, Nagatsuka Y (1984) Shear flow rheological properties of vinylon- and glass-fiber reinforced polyethylene melts. Rheol Acta 23:20–30

Kitano T, Kataoka T, Shirota T (1981) An empirical equation of the relative viscosity of polymer melts filled with various inorganic fillers. Rheol Acta 20:207–209

Laun HM (1984) Orientation effects and rheology of short glass fiber-reinforced thermoplastics. Colloid Polym Sci 262:257–269

Lipscomb GG, Denn MM, Hur DU, Boger DV (1988) The flow of fibers suspensions in complex geometries. J Non-Newt Fluid Mech 26:297–325

Mackaplow MB, Shaqfeh ESG (1996) A numerical study of the rheological properties of suspensions of rigid, non-Brownian fibres. J Fluid Mech 329:155–186

Mewis J, Metzner AB (1974) The rheological properties of suspensions of fibres in Newtonian fluids subjected to extensional deformations. J Fluid Mech 62:593–600

Papanastasiou TC, Alexandrou AN (1987) Isothermal extrusion of non-dilute fiber suspensions. J Non-Newt Fluid Mech 25:313–328

Phan-Thien N, Graham AL (1991) A new constitutive model for fiber suspensions: flow past a sphere. Rheol Acta 30:44–57

Ranganathan S, Advani SG (1991) Fiber-fiber interactions in homogeneous flows of non-dilute suspensions. J Rheol 35: 1499–1522

Shaqfeh ESG, Fredrickson GH (1990) The hydrodynamic stress in a suspension of rods. Phys Fluids A 2:7–24

Shaqfeh ESG, Koch DL (1990) Orientational dispersion of fibers in extensional flows. Phys Fluids A 2:1077–1093

Souloumiac B (1996) Etude rhéologique, modélisation et simulation numérique de l'écoulement des thermoplastiques chargés de fibres courtes. PhD Thesis, Ecole des Mines de Paris, France

Tang L, Altan MC (1995) Entry flow of fiber suspensions in a straight channel. J Non-Newt Fluid Mech 56:183–216

Villemaire JP, Agassant JF (1984) Apparent viscosity measurements using a capillary viscometer with preshearing. Polym Proc Eng 1:223–232

Vincent M, Agassant JF (1991) Predicting fiber orientation in injection molding. In: Utracki LA (ed) Two-phase polymer systems, progress in polymer processing. Chap. 11. Hanser, Munich

Wang MW, Cheau TC (1991) A constitutive approach for studying concentrated suspensions of rigid fibres in a non-Newtonian Ellis fluid. J Chinese Institute of Eng 14:483–493